IL NUOVO CIMENTO **43 C** (2020) 36
DOI 10.1393/ncc/i2020-20036-1

Colloquia: IFAE 2019

First evidence of double-parton scattering in same-sign WW production at CMS

V. Mariani for the CMS Collaboration
INFN, Sezione di Perugia - Perugia, Italy

received 8 June 2020

Summary. — The search for the same-sign WW production via double-parton scattering is presented, based on study of proton-proton collision data collected at $\sqrt{s} = 13\,\text{TeV}$, using dimuon and electron-muon final states with the CMS experiment. First evidence for WW production via double-parton scattering, with a significance of 3.9 standard deviations, is presented. The measured inclusive cross-section is 1.41 ± 0.28 (stat)± 0.28 (syst) pb.

1. – What is double-parton scattering

An interaction where two hard scatters between two independent partons occur, within the same proton-proton collision, is indicated as Double Parton Scattering (DPS) [1, 2]. Assuming that both the partonic cross-sections and the transverse and longitudinal parts of the PDF terms factorize, the DPS cross-section can be written in a simplified model [3] as

$$\sigma_{DPS} = \frac{n}{2}\frac{\sigma_A \sigma_B}{\sigma_{eff}}, \tag{1}$$

where A and B represent the Single Parton Scattering (SPS) processes, and σ_A and σ_B are their respective production cross-sections. The factor n is equal to unity if processes A and B are the same, and is equal to 2 otherwise. The parameter σ_{eff}, the effective cross-section of DPS processes, is related to the extent of the parton distribution in the plane orthogonal to the direction of motion of the protons.

σ_{eff} has been measured at different hadron colliders and center-of-mass energies in a variety of final-state processes with comparatively large uncertainties (30%). Its value ranges between 15 and 26 mb for processes involving a vector boson [4, 5].

One of the most promising processes to study DPS is the case in which the two hard scatterings lead to the production of same-sign W bosons (ssWW) [6]. The corresponding SPS production of ssWW includes two additional partons, therefore it is suppressed. The

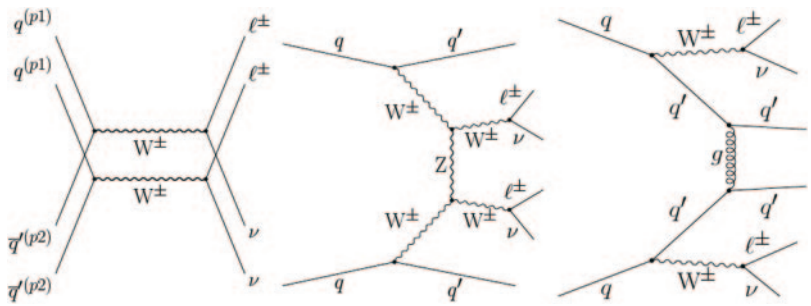

Fig. 1. – The left diagram shows a ssWW DPS event, while the centre and right ones show possible topologies of SPS ssWW production.

processes involved in the $W^{\pm}W^{\pm}$ production are shown in fig. 1: on the left, the DPS mechanism and on the center and on the right the SPS modes.

The absence of jets in the ssWW production via DPS at LO provides an additional handle to reduce the contributions from the SPS backgrounds. Moreover, when both W bosons decay leptonically, this event exhibits a clean final state in the detector, and the excellent reconstruction and resolution of leptons in the CMS detector provides an accurate measurement of the ssWW DPS cross-section.

A search for the production of WW via DPS was reported in the past by the CMS Collaboration using pp collisions at $\sqrt{s} = 8\,\text{TeV}$, setting an upper limit of 0.32 pb on its production cross-section at 95% confidence level [7].

An increased production cross-section at $\sqrt{s} = 13\,\text{TeV}$ and a larger data set collected using the CMS detector allow a more detailed study of this interesting physics process. This paper presents a measurement of the ssWW production via DPS performed with pp collision data, recorded using the CMS experiment at a center-of-mass energy of 13 TeV in 2016 and 2017 [8]. The analysis focuses on the leptonic decay of the W bosons in final states consisting of a same charge electron-muon ($e\mu$) or dimuon ($\mu\mu$) pair. The analyzed data sample corresponds to an integrated luminosity of $77.4\,\text{fb}^{-1}$.

2. – Analysis strategy

The signal region definition is based on the presence of two same-sign isolated leptons and a certain amount of missing transverse momentum (p_T^{miss}) originating from the neutrinos in the W boson decays. Leptons are required to originate from the primary vertex of the event, identified as the reconstructed vertex with the largest value of $\sum p_T^2$ of the outgoing physics objects. Tight selection criteria have been applied to both electrons and muons in order to distinguish "prompt" leptons, coming from W, Z, or τ lepton decays, from "non-prompt" leptons, originating from heavy-quark decays or quark and gluon jets incorrectly reconstructed as leptons.

Events are selected by requiring exactly two leptons of the same charge, $e^{\pm}\mu^{\pm}$ or $\mu^{\pm}\mu^{\pm}$, with p_T greater than 25(20) GeV for the leading (subleading) lepton, and $|\eta| < 2.5$ (2.4) for electrons (muons). Events are vetoed if there are additional leptons fulfilling looser identification and isolation requirements. A conservative low threshold of 15 GeV is applied to p_T^{miss}, reducing the contributions from QCD multijet production. The signal process involves no jet activity at LO although around 25% of signal events contain at least one reconstructed jet with $p_T^{jet} > 30\,\text{GeV}$ within $|\eta_{jet}| < 2.5$. To ensure high signal

efficiency, a requirement of at most one such jet is imposed, while processes with b quark jets are suppressed by rejecting events with at least one b-tagged jet having $p_T^{bjet} > 25\,\mathrm{GeV}$ and $|\eta_{bjet}| < 2.4$.

3. – Background estimation

Background processes can be separated into two categories: processes involving same-charge lepton pairs from leptonic decays of bosons produced in the hard scattering and processes that resemble the production of prompt, same-charge lepton pairs.

The first category includes the WZ, Wγ, Zγ, ZZ, WW production via SPS and WWW processes. In all of them the boson decay leptonically and eventual additional leptons could be either out of detector acceptance or does not pass the identification criteria. In the case of γ presence in association with the W or Z bosons, it contributes via asymmetric conversions into lepton pairs inside the detector. All these background components are estimated from MC simulation.

The second background category includes both non-prompt lepton background in which one or two of the selected leptons do not originate from the decay of a massive boson from the hard scattering, dominated by W+jets and QCD multijet events, and misassignment of the charge of an electron in the reconstruction, dominated by $Z \to \tau\tau$ events with leptonic decay of the τ. The lepton misidentification rate, defined as the probability of a "loose" non-prompt lepton to pass the "tight" lepton selection criteria, is estimated directly from the data in a sample dominated by non-prompt leptons and it is measured separately for electrons and muons as a function of the lepton p_T and $|\eta|$. Similarly the probability for the charge of a lepton to be incorrectly reconstructed is calculated and applied to the selected opposite-charge dilepton events in data, measured in Z $\to ee$ events as the ratio of same-charge to opposite-charge dilepton events. The values are <1% in the whole range for electrons, while it is negligible for muons.

4. – Multivariate classifier training

After the initial analysis strategy event selection, the major background contributions arise from WZ production and processes with non-prompt leptons. To achieve a good separation between the signal and these two background components, two different multivariate analysis (MVA) classifiers are trained using a set of kinematic variables.

The WZ background is kinematically very similar to the signal, because they are both characterised by two prompt leptons with similar p_T spectra, moderate p_T^{miss} and no hadronic activity. The main difference between the signal and WZ production is that in the latter the bosons share a Lorentz boost along the z-axis, while the bosons in the signal process are almost uncorrelated.

In the case of non-prompt lepton production, dominated by W+jets and QCD multijet processes, the kinematic differences with respect to the signal are larger but these processes have production cross-sections orders of magnitude grater than that for the signal process. Therefore, even with a low probability of passing the event selection criteria, the impact of these background processes is considerable.

A framework based on boosted decision trees (BDT) combines this information to discriminate between the signal and the background events, defining a set of eleven input variables to train the BDTs, based on lepton and event kinematic. These variables

have been chosen since they all show significant discrimination between the signal and background processes:

- $p_T^{\ell_1}$, $p_T^{\ell_2}$ and p_T^{miss}: transverse momenta of the two leptons and missing transverse momentum.
- $\eta_{\ell_1} \cdot \eta_{\ell_2}$ and $|\eta_{\ell_1} + \eta_{\ell_2}|$: product and absolute sum of pseudorapidities of the two leptons.
- $m_T(\ell_1, p_T^{miss})$ and $m_T(\ell_1, \ell_2)$: transverse mass of the leading lepton and p_T^{miss} and transverse mass of the leading and subleading leptons.
- $|\Delta\phi(\ell_1, \ell_2)|$, $|\Delta\phi(\ell_2, p_T^{miss})|$ and $|\Delta\phi(\ell_1\ell_2, \ell_2)|$: azimuthal angular separation between the leptons, the subleading lepton and p_T^{miss} and between the dilepton system and the subleading lepton.
- $m_{T2}(\ell_1, \ell_2)$: "stransverse mass" of the dilepton and p_T^{miss} system, defined as $m_{T2} = \min_{\vec{p}_T^{miss(1)}+\vec{p}_T^{miss(2)}=\vec{p}_T^{miss}} [\max(m_{\mathrm{T}}^{(1)}, m_{\mathrm{T}}^{(2)})]$, where $\vec{p}_T^{miss}$ has two components $\vec{p}_T^{miss(1)}$ and $\vec{p}_T^{miss(2)}$ to produce the transverse masses $m_T^{(1)}$ and $m_T^{(2)}$ with the corresponding lepton. When both leptons and both neutrinos originate from mother particles of equal mass, the $m_{T2}(\ell_1, \ell_2)$ variable shows an end point at the mother particle mass.

The two classifiers are mapped into a single two-dimensional (2D) classifier by combining contiguous regions in the 2D plane of the two separate classifiers. These regions are chosen to optimize the constraining power of the maximum likelihood fit. In total, the 2D plane is split into 15 bins, on which the final fit is performed.

Events are analyzed separately in the two distinct lepton flavour channels and the two charge configurations ($++$ and $--$). This classification increases the sensitivity of the analysis because the signal process is expected to be enhanced in the $\ell^+\ell^+$ configuration, while the background processes exhibit more symmetry between the two charges.

5. – Systematic uncertainties

Various sources of systematic uncertainties, experimental and theoretical, can be grouped into two categories. The first type changes the overall normalization of one or more processes while the second one can change both the normalization and the shape of the final 1D classifier distribution.

The uncertainty in the integrated luminosity is 2.5 (2.3)% for the 2016 (2017) data-taking period [9, 10]. The dominant source of experimental systematic uncertainty is associated with the method adopted for the estimation of non-prompt lepton contributions. A normalization uncertainty of 40 (25)% for the $e^\pm\mu^\pm$ ($\mu^\pm\mu^\pm$) final state is applied. A 30% normalization uncertainty is applied to the "charge misidentification" background in the $e^\pm\mu^\pm$ final state. Normalization uncertainties for the main backgrounds estimated from simulation are derived in dedicated 3 (4) lepton control regions for the WZ (ZZ) processes, with scale factors that are measured to be 1.01 ± 0.16 and 0.97 ± 0.06, respectively. The normalization uncertainties are estimated to be 16 (6)% for the WZ (ZZ) process. A 50% normalization uncertainty is applied to all other simulated backgrounds, accounting for the theoretical uncertainties in the predicted cross-sections and the lack of proper control samples in the data. A 5% shape uncertainty is applied

to the simulation-derived backgrounds, coming from the data/MC comparison, while the uncertainty in the pileup modeling is 1%. The uncertainty in the b tagging is considerably smaller than the statistical uncertainty in the simulated samples and is therefore neglected. The acceptance effect of the uncertainty in the jet energy scale is 2% in the signal and the simulated background samples and is considered fully correlated among all channels. The trigger efficiency uncertainty associated with the combination of single-lepton and dilepton triggers is 1–2%, whereas the uncertainty in the data-to-simulation scale factors for the lepton selection is 2–3%. Finally, the statistical uncertainty arising from the limited number of events in the simulated samples is included independently for each bin of the final discriminant distribution for each final state and the two data-taking periods.

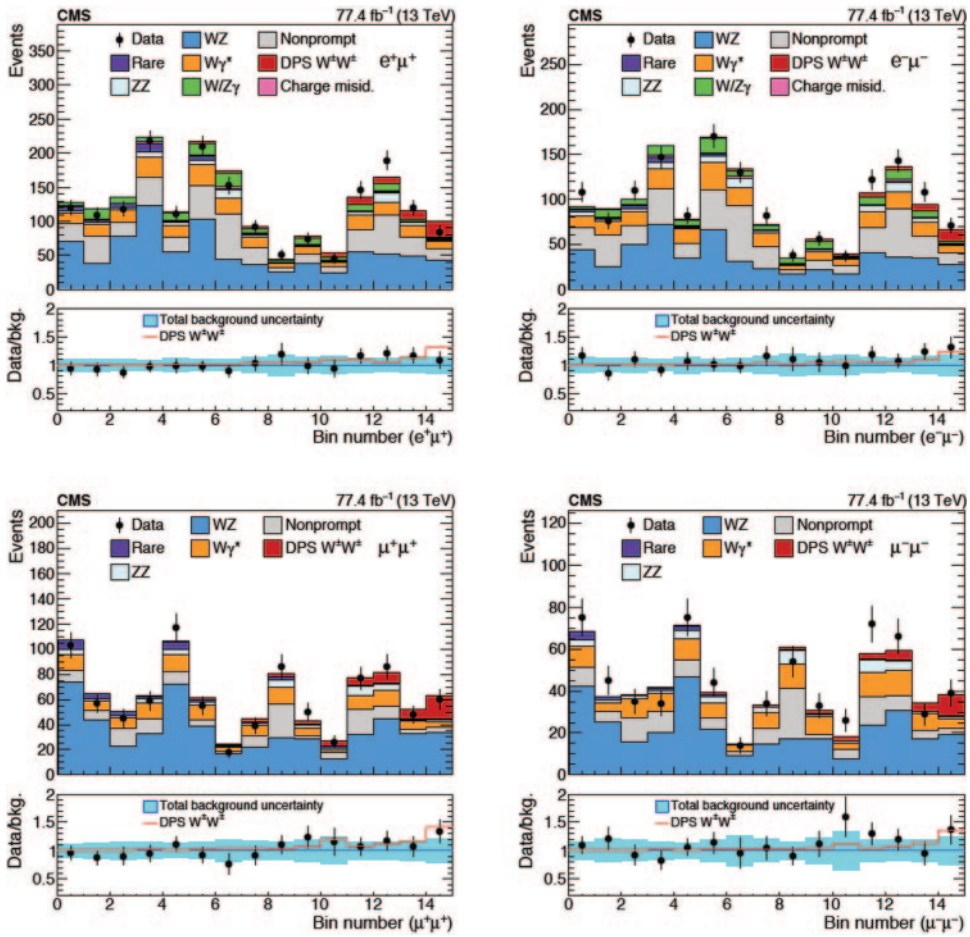

Fig. 2. – Distribution of the final BDT classifier output for $e\mu$ (upper) and $\mu\mu$ (lower) final states, in the positive (left) and negative (right) charge configurations. Observed data are shown in black markers while the backgrounds and signal are shown in colored histograms with their postfit yields. The bottom panels show the ratio of data to the sum of all background contributions in the black markers along with the signal shown using a red line. The band represents the background uncertainty, including both the statistical and systematic components [8].

TABLE I. – *Results obtained from the maximum likelihood fit to the final classifier distribution.*

	Value	Significance (standard deviation)
$\sigma^{PYTHIA}_{DPSWW,exp}$	1.92 pb	5.2
$\sigma^{factorised}_{DPSWW,exp}$	0.87 pb	2.5
$\sigma_{DPSWW,obs}$	1.41 ± 0.28 (stat) ± 0.28 (syst) pb	3.9
σ_{eff}	$12.7^{5.0}_{2.9}$ mb	–

6. – Results

Results are obtained after combining all the background and signal processes in four different configurations, $e^+\mu^+$, $e^-\mu^-$, $\mu^+\mu^+$, $\mu^-\mu^-$, resulting in four independent distributions of the final BDT classifier. The final maximum likelihood fit is performed simultaneously in these distinct categories. The classification of events into the two charge configurations increases the sensitivity of the analysis by 10%.

In fig. 2 the distribution of the final BDT classifier in the two charge configurations, $e^\pm\mu^\pm$ channel in the upper row and $\mu^\pm\mu^\pm$ in the bottom row, are shown.

For this analysis, two predicted cross-sections are used. The PYTHIA event generator with the CP5 tune gives a cross-section of 1.92 pb. Alternatively, using eq. (1) with the highest-order cross-section for inclusive W boson production and decay at next-to-NLO accuracy in QCD along with $\sigma_{eff} = 20.7 \pm 6.6$ mb, just basing on a measurement of final state containing W boson [11], results in an expected cross section for the inclusive DPS WW process of 0.87 ± 0.28 pb.

The following quantities are obtained from the simultaneous fit to the final BDT classifier in the four lepton charge and flavour combinations:

- the expected significance assuming the signal process follows the PYTHIA kinematics with the input cross-section as $\sigma^{PYTHIA}_{DPSWW,exp}$;
- the expected significance assuming the signal process exhibits PYTHIA-like kinematics with a production cross-section, $\sigma^{factorised}_{DPSWW,exp}$, extracted based on the factorization approach using the inclusive W production cross-section and value of σ_{eff} mentioned above;
- the observed cross-section $\sigma_{DPSWW,obs}$ and the corresponding significance, assuming PYTHIA-like kinematics, independent of the assumed cross-section;
- σ_{eff} using the inclusive W production cross-section and $\sigma_{DPSWW,obs}$.

A maximum likelihood fit is performed separately for different lepton charge configurations and their combination. The values obtained for the DPS WW cross-section are then extrapolated to the inclusive WW phase space. The numbers extracted from the maximum likelihood fit to the final classifier distribution for the combination of the $\ell^+\ell^+$ and $\ell^-\ell^-$ final states are shown in table I.

7. – Summary

A study of WW production from double-parton scattering (DPS) processes in proton-proton collisions at $\sqrt{s} = 13\,\text{TeV}$ has been presented. The analyzed data set corresponds to an integrated luminosity of $77.4\,\text{fb}^{-1}$, collected using the CMS detector in 2016 and 2017 at the LHC. The WW candidates are selected from $e^{\pm}\mu^{\pm}$ and $\mu^{\pm}\mu^{\pm}$ events with moderate missing transverse momentum and low jet multiplicity. Multivariate classifiers based on boosted decision trees are used to discriminate between the signal and the dominant background processes. A maximum likelihood fit is performed to extract the signal cross-section, which is compared to the predictions from simulation and from an approximate factorization approach. A measurement of the DPS WW cross-section is achieved for the first time, and a cross-section of 1.41 ± 0.28 (stat) $\pm\, 0.28$ (syst) pb is extracted with an observed significance of 3.9 standard deviations with respect to the background-only hypothesis. This cross-section leads to an effective cross-section parameter of $\sigma_{eff} = 12.7^{5.0}_{2.9}\,\text{mb}$. This results constitute the first evidence for WW production from DPS.

REFERENCES

[1] Bartalini P. and Fanó L., *Proceedings of the 1st International Workshop on Multiple Partonic Interactions at the LHC (MPI08)*, DESY-PROC-2009-06.
[2] Astalos R. *et al.*, *Proceedings of the Sixth International Workshop on Multiple Partonic Interactions at the Large Hadron Collider* (2015) arXiv:1506.05829.
[3] Treleani D., *Phys. Rev. D*, **76** (2007) 07600.
[4] CDF Collaboration, *Phys. Rev. Lett.*, **79** (1997) 584.
[5] LHCb Collaboration, *JHEP*, **07** (2016) 052.
[6] Gaunt J. R., Kom C. H., Kulesza A. *et al.*, *Eur. Phys. J. C*, **69** (2010) 53.
[7] CMS Collaboration, *JHEP*, **02** (2018) 032.
[8] CMS Collaboration, *Evidence for WW production from double-parton interactions in proton-proton collisions at* $\sqrt{s} = 13$ *TeV*, submitted to *Eur. Phys. J. C*, arXiv:1909.06265
[9] CMS Collaboration, *CMS luminosity measurements for the 2016 data-taking period*, CMS-PAS-LUM-17-001, `https://cds.cern.ch/record/2257069`.
[10] CMS Collaboration, *CMS luminosity measurement for the 2017 data-taking period at* $\sqrt{s} = 13$ *TeV*, CMS-PAS-LUM-17-004, `https://cds.cern.ch/record/2621960`.
[11] CMS Collaboration, *JHEP*, **03** (2014) 032.